

# UC Berkeley

## UC Berkeley Previously Published Works

### Title

Highly Enhanced Curie Temperature in Ga-Implanted Fe<sub>3</sub>GeTe<sub>2</sub> van der Waals Material

### Permalink

<https://escholarship.org/uc/item/4k29t7m0>

### Journal

Advanced Quantum Technologies, 3(4)

### ISSN

2511-9044

### Authors

Yang, Mengmeng  
Li, Qian  
Chopdekar, Rajesh V  
[et al.](#)

### Publication Date

2020-04-01

### DOI

10.1002/qute.202000017

Peer reviewed

# Highly enhanced Curie temperature in Ga-implanted Fe<sub>3</sub>GeTe<sub>2</sub> van der Waals material

*Mengmeng Yang<sup>+</sup>, Qian Li<sup>+\*</sup>, Rajesh V. Chopdekar, Camelia Stan, Stefano Cabrini, Jun Woo Choi, Sheng Wang, Tianye Wang, Nan Gao, Andreas Scholl, Nobumichi Tamura, Chanyong Hwang, Feng Wang, and Ziqiang Qiu\**

Dr. Mengmeng Yang, Dr. Qian Li, Sheng Wang, Tianye Wang, Dr. Nan Gao, Prof. Feng Wang, Prof. Ziqiang Qiu

Department of Physics, University of California, Berkeley, California 94720, United States  
Email: qianli2015@berkeley.edu; qiu@berkeley.edu

Dr. Rajesh V. Chopdekar, Dr. Camelia Stan, Dr. Stefano Cabrini, Dr. Andreas Scholl, Dr. Nobumichi Tamura

Advanced Light Source and Molecular Foundry, Lawrence Berkeley National Laboratory, Berkeley, California 94720, United States

Dr. Jun Woo Choi

Center for Spintronics, Korea Institute of Science and Technology, Seoul 02792, Korea

Prof. Chanyong Hwang

Korea Research Institute of Standards and Science, Yuseong, Daejeon 305-340, Republic of Korea

Keywords: van der Waals magnetism, Curie temperature enhancement, Photoemission Electron Microscopy, Ga implantation

## Abstract

Among many efforts in the research of van der Waals (vdW) magnetic materials, increasing the Curie temperature above room temperature has been at the center of research in developing spintronics technology using vdW materials. Here we report an effective and reliable method of increasing the Curie temperature of ferromagnetic Fe<sub>3</sub>GeTe<sub>2</sub> vdW materials by Ga implantation. We find that implanting Ga into Fe<sub>3</sub>GeTe<sub>2</sub> by the amount of 10<sup>19</sup> Ga Å<sup>-3</sup> could greatly enhance the Fe<sub>3</sub>GeTe<sub>2</sub> Curie temperature by almost 100%. Spatially resolved microdiffraction and element-resolved x-ray absorption spectroscopy show little changes in the Fe<sub>3</sub>GeTe<sub>2</sub> crystal structure and Fe valence state. In addition, the Ga implantation changes the Fe<sub>3</sub>GeTe<sub>2</sub> magnetization from out-of-plane direction at low temperature to in-plane direction at high temperature. Our result opens a new opportunity for tailoring the magnetic properties of vdW materials beyond room temperature.

The discovery of intrinsic magnetic long-range order in two dimensional (2D) van der Waals (vdW) materials<sup>[1,2]</sup> opened up enormous opportunities for both fundamental research and spintronic applications.<sup>[3,4]</sup> Great effort has been devoted along two directions in the last a few years. One is to integrate magnetization with other physical quantities aiming to control each other, such as the control of the interlayer coupling by electric field<sup>[5,6]</sup> and doping<sup>[7]</sup>, gate-modulation of the magnetism and magneto-optics<sup>[8]</sup>, and pressure-induced spin-lattice coupling<sup>[9]</sup> and spin reorientation transition,<sup>[10]</sup> etc. The other direction is to enhance the Curie temperature ( $T_C$ ) of vdW materials above room temperature for future spintronics devices. Noticing that most of the vdW magnetic materials have a  $T_C$  well below room temperature, the second direction is particularly important and urgent for future technological applications of vdW magnetic materials.

Recently, there have been several different approaches that successfully increase the  $T_C$  of vdW materials above room temperature even though the underlying mechanism remains unclear. One approach is to grow vdW thin films using Molecular Beam Epitaxy (MBE). For example, it was reported that single-layer MBE-grown  $VSe_2$ <sup>[11]</sup> has a  $T_C$  above room temperature and a corresponding giant magnetic moment ( $\sim 15\mu_B$  per unit cell). Room temperature magnetic order of MBE-grown  $MnSe_x$  was also reported<sup>[12]</sup> with caution because of the complicated  $MnSe_x$  phase diagram. The second approach is to enhance  $T_C$  by ionic gating although it is difficult to distinguish the effects between the energy band shift and the intercalation of lithium ions.<sup>[13]</sup> Finally, it was reported that patterning vdW magnetic flakes into microstructures using focused ion beam (FIB) could lead to a  $T_C$  above room temperature.<sup>[14]</sup> Again it is unclear on the underlying mechanism as a pure finite size effect or as a possible Ga doping from the FIB. Regardless of the underlying mechanism, the above results indicate that the  $T_C$  of vdW magnetic material is very sensitive to its environment,

making it very promising to tune the  $T_C$  of vdW magnetic material by chemical doping. In this paper, we report an effective and reliable method to tune the  $T_C$  of  $\text{Fe}_3\text{GeTe}_2$  vdW materials from the bulk value of 230 K to as high as 450 K by controlling the fluence of Ga irradiation on the  $\text{Fe}_3\text{GeTe}_2$ .

Figure 1b shows the image of one 170 nm thick  $\text{Fe}_3\text{GeTe}_2$  flake onto which a series of square-shaped areas ( $4\ \mu\text{m} \times 4\ \mu\text{m}$ ) had been exposed to  $\text{Ga}^+$  irradiation (30keV, 10pA) with different exposure time as described in the experimental section under exactly the same condition. In this way, we can single out the effect of Ga irradiation fluence on the  $T_C$  enhancement by eliminating other factors such as the square size, sample thickness, and  $\text{Ga}^+$  voltage/current, etc. Figure 1c-f show the magnetic contrast above room temperature from four micropatterns with  $\text{Ga}^+$  exposure time of 10 s, 14 s, 18 s and 30 s as measured with x-ray photoemission electron microscopy (PEEM). We find that all four  $\text{Fe}_3\text{GeTe}_2$  micropatterns exhibit in-plane magnetization forming a vortex state at room temperature (300 K) and the surrounding unexposed  $\text{Fe}_3\text{GeTe}_2$  materials show the expected zero magnetic contrast, indicating that  $\text{Ga}^+$  exposure has locally enhanced the  $T_C$  of  $\text{Fe}_3\text{GeTe}_2$  from its bulk value of 230 K to above room temperature. The contrast is reversed when changing the x-ray polarization from left- to right-circularly polarizations, indicating that the origin of the contrast is magnetic (see discussions below). The magnetic vortex contrast disappears at temperatures higher than room temperature (indicated by the blue arrows in Figure 1c-f), further demonstrating an enhanced  $T_C$  above room temperature.

Figure 1. a) Crystal structure (side view) of  $\text{Fe}_3\text{GeTe}_2$ . b) Scanning Electron Microcopy image of a  $\text{Fe}_3\text{GeTe}_2$  flake (yellow color) on a silicon substrate (orange color). Arrays of squares ( $4\mu\text{m}\times 4\mu\text{m}$ ) on the flake are exposed to Ga irradiation with different time with the squares marked by black, red, blue and pink color exposed by 10 s, 14 s, 18 s and 30 s, respectively. c)-f) Temperature-dependent magnetic domains from the four squares marked in b). Blue arrows indicate the corresponding  $T_C$  where the magnetic contrast disappears. Red arrow at the bottom of the figure indicates the incident direction of the circularly polarized x-rays.

Figure 2a shows the temperature-dependent magnetic contrast of the vortices with different  $\text{Ga}^+$  exposure time. We extrapolate the  $T_C$  value from the temperature at which magnetic contrast disappears. For 20-s and 30-s  $\text{Ga}^+$  exposure time, the  $T_C$  value is obviously above 390 K which is the highest achievable temperature of the cryogenic PEEM sample holder. For these two cases, we estimate the  $T_C$  by extracting the zero-contrast temperature from the temperature-dependent magnetic contrast below 390 K. The result (Figure 2b)

shows unambiguously a monotonic increase of  $T_C$  up to 450 K with increasing the  $\text{Ga}^+$  exposure time, demonstrating the effective method of tuning the  $T_C$  of  $\text{Fe}_3\text{GeTe}_2$  by controlling the Ga irradiation time.

After confirming the enhancement of  $T_C$  by  $\text{Ga}^+$  irradiation, the next question is what is the effect of  $\text{Ga}^+$  irradiation on  $\text{Fe}_3\text{GeTe}_2$ ? Obviously, the high energy  $\text{Ga}^+$  should sputter away some materials (Pd covering layer and some  $\text{Fe}_3\text{GeTe}_2$ ) off the sample even though the Ga exposure time is short. Detailed depth calibration shows that the Pd covering layer was indeed sputtered away from the sample (Figure S1, Supporting Information). In addition to the sputtering effect, high energy  $\text{Ga}^+$  irradiation has been reported to also result in amorphization or structural change of 2D materials.<sup>[15,16,17]</sup> A recent experiment<sup>[15]</sup> shows that a Ga dose of  $3.1 \times 10^{15}$  ions  $\text{cm}^{-2}$ , which is similar to our case of 10 s exposure time (Ga dose  $3.9 \times 10^{15}$  ions  $\text{cm}^{-2}$ ), to a single layer graphene could amorphize or change  $\sim 1/3$  layer into other structures. To search for any structural change of the  $\text{Fe}_3\text{GeTe}_2$  crystal due to Ga irradiation, we performed microdiffraction measurement. We find that the Laue diffraction from the  $\text{Ga}^+$  exposed area (Figure 2e) exhibits identical pattern as the un-exposed area (Figure 2f). Detailed analysis of the Laue pattern allows a quantitative mapping (Figure 2d) of the lattice strain in the out-of-plane direction.<sup>[18]</sup> The result shows that the variation of the out-of-plane lattice constant is no more than 0.2%. However, this microdiffraction result does not rule out the existence of small amount of amorphous or structural changed  $\text{Fe}_3\text{GeTe}_2$  because the Laue diffraction is from the whole  $\text{Fe}_3\text{GeTe}_2$  flake. More likely, our result suggests that most of  $\text{Ga}^+$  exposed  $\text{Fe}_3\text{GeTe}_2$  retains its original single-crystalline structure with small amount being changed into amorphous or structurally damaged  $\text{Fe}_3\text{GeTe}_2$ . It is difficult to quantify the amount of the amorphous layer and the percentage of remaining crystalline  $\text{Fe}_3\text{GeTe}_2$  within this amorphous layer. We estimate a possible 10-30 nm amorphous or structurally changed layer in our sample according to Ga irradiation result on a

range of different materials.<sup>[19]</sup> From the point of view of magnetism, magnetic vortex state could be formed spontaneously only above a critical thickness,<sup>[14, 20]</sup> the amorphous or structurally changed layer alone seems unlikely to form the magnetic vortex state. Therefore, the magnetic vortex state is more likely contributed from both the amorphous or structurally changed surface layer and the single crystalline Fe<sub>3</sub>GeTe<sub>2</sub>. Another factor which should be considered is the strain effect. Theoretical calculation<sup>[ 21 ]</sup> shows that the perpendicular magnetic anisotropy in single layer Fe<sub>3</sub>GeTe<sub>2</sub> could be enhanced by biaxial tensile strains and be weakened by compressive strains. The latter could be a plausible mechanism for the observed in-plane magnetization in Figure 1. Obviously, more investigation on the Ga irradiated Fe<sub>3</sub>GeTe<sub>2</sub> layer (e.g. thickness, amorphization level, structure change, defects amount etc.) is needed in the future with nanometer resolved structural characterizations.

Besides the sputtering and amorphization effects, some tiny amount of the high energy Ga ions could also penetrate and be implanted inside the Fe<sub>3</sub>GeTe<sub>2</sub>. Estimated from our calculation (Figure S2, Supporting Information), the mean Ga implantation depth is about 14 nm. Therefore the 10-30 s exposure time at 10 pA in Figure 1 corresponds to  $2.8-8.4 \times 10^{-3}$  Ga Å<sup>-3</sup> (assuming 100% incident Ga were implanted into Fe<sub>3</sub>GeTe<sub>2</sub>) which is much less than the Fe atoms inside Fe<sub>3</sub>GeTe<sub>2</sub>. We then did chemical analysis of the Ga and Fe atoms in the sample by taking element-resolved x-ray absorption spectroscopy (XAS) at the Ga absorption edge (Figure 2g) and the Fe absorption edge (Figure 2h), respectively. The high sensitivity of XAS allows the detection of tiny amount of Ga inside the sample. Indeed, the presence of the Ga XAS from the Ga<sup>+</sup> exposed area confirms the existence of Ga inside the sample. The increased Ga intensity with Ga<sup>+</sup> exposure time suggests an increased concentration of Ga inside Fe<sub>3</sub>GeTe<sub>2</sub> (Figure 2g). The XAS from the Fe absorption edge, however, show little change with the Ga<sup>+</sup> exposure time (Figure 2h). Therefore we conclude that either the amorphized Fe<sub>3</sub>GeTe<sub>2</sub> has almost identical Fe spectra as in un-irradiated Fe<sub>3</sub>GeTe<sub>2</sub>,<sup>[22]</sup> or Ga

amount is too tiny to change the valence state of the Fe atoms in  $\text{Fe}_3\text{GeTe}_2$ . Then the interesting question is whether the ferromagnetic state shown in Figure 1 is from the majority Fe atoms in  $\text{Fe}_3\text{GeTe}_2$  or from the tiny amount of Fe atoms around the implanted Ga ions? We measured the X-ray Magnetic Circular Dichroism (XMCD) by taking the difference of XAS for left- and right-circularly polarized x-rays. Figure 2i shows representative XMCD result taken from different locations of a magnetic vortex at room temperature. As expected, the XMCD signals from opposite magnetizations of the magnetic vortex exhibit opposite signs and the XMCD outside the  $\text{Ga}^+$  exposed region shows zero XMCD signal, demonstrating clearly the ferromagnetic origin of the contrast in Figure 1c-1f. The single peak of Fe XMCD at  $L_3$  and  $L_2$  edges also rules out the ferromagnetic origin from any possible Fe oxides such as  $\gamma\text{-Fe}_2\text{O}_3$  and  $\text{Fe}_3\text{O}_4$ .<sup>[23]</sup> Most importantly, the XMCD magnitude (4.8%) is similar to the XMCD magnitude from unexposed  $\text{Fe}_3\text{GeTe}_2$ <sup>[14]</sup>, showing that the ferromagnetic order is from the majority of the Fe atoms in  $\text{Fe}_3\text{GeTe}_2$  rather than from tiny amount of the Fe atoms around the implanted Ga ions (see part 3 in Supporting Information). Then all the above results show that regardless of the detailed effects of Ga implantation on  $\text{Fe}_3\text{GeTe}_2$  crystal, a tiny amount Ga implantation increases the  $T_C$  of the  $\text{Fe}_3\text{GeTe}_2$  by ~100%, demonstrating the sensitive dependence of the  $\text{Fe}_3\text{GeTe}_2$   $T_C$  on its environmental change. Although it is too early to identify the underlying mechanism unambiguously, several possible mechanisms were discussed (see part 4 in Supporting Information). Despite the fact that Ga implantation could damage the crystal structure of the materials, the enhanced Curie temperature beyond room temperature may still create application potentials to devices which do not require perfect crystal structure of vdW materials.<sup>[ 24,25,26,27]</sup>



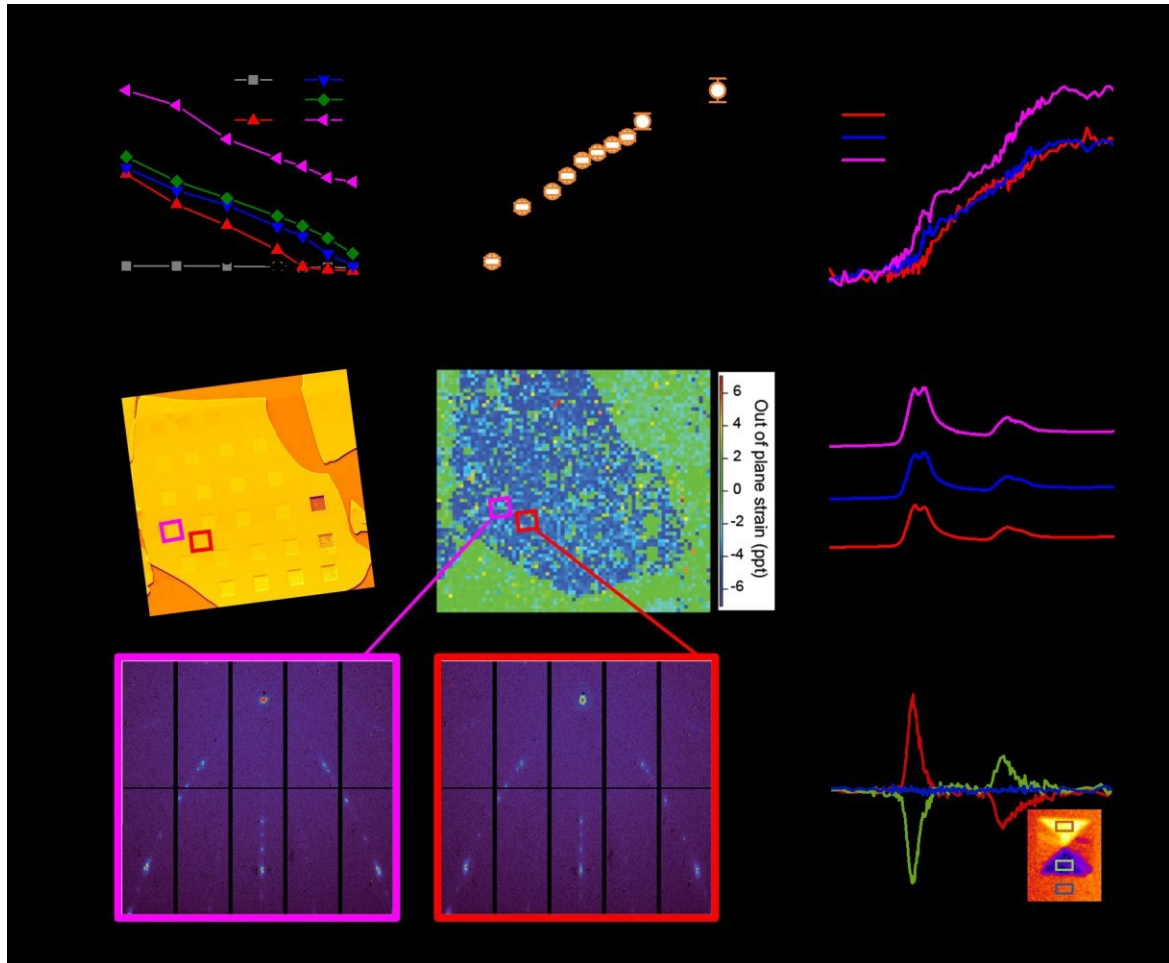


Figure 2. a) Magnetization contrast as a function of temperature from  $\text{Fe}_3\text{GeTe}_2$  with different Ga exposure time. b) Summarized Curie temperature as a function of Ga exposure time. c) Scanning Electron Microcopy image of the Ga-milled  $\text{Fe}_3\text{GeTe}_2$  flake. d) The out-of-plane strain mapping obtained from micro-diffraction. Selected Laue patterns from e) 30s-Ga exposed f) un-exposed area. Selected XAS at g) Ga edge and h) Fe edge from  $\text{Fe}_3\text{GeTe}_2$  with various exposure time. i) XMCD spectra from a magnetic vortex formed in a Ga-exposed  $\text{Fe}_3\text{GeTe}_2$  square at RT.

Notice that the magnetic vortex state in Figure 1 has in-plane magnetization and the Ga unexposed  $\text{Fe}_3\text{GeTe}_2$  has out-of-plane magnetization with stripe domains<sup>[14]</sup> (below bulk  $T_C=230\text{K}$ ). Then the result in Figure 1 shows that the Ga implantation not only increases the  $T_C$  but also changes the easy magnetization direction of  $\text{Fe}_3\text{GeTe}_2$  (see part 5 in Supporting Information). Thus, to explore the in-plane magnetic properties of Ga-implanted  $\text{Fe}_3\text{GeTe}_2$ ,

we varied the shape of Ga implanted microstructures and imaged domain changes after applying an in-plane magnetic field. Different shapes of microstructures allow study of the competition between shape anisotropy energy and magnetocrystalline energy. We implanted a 5- $\mu\text{m}$  diameter circular area (30 keV, 10 pA, 15 s) and took magnetic images at both room temperature and low temperature. Different from the square shapes in Figure 1 which favors the magnetization along the four directions parallel to the edges, we found the circular shape has magnetization direction of the magnetic vortex circulates continuously rather than along any certain directions (Figure 3a and Figure 3c). This result shows the  $\text{Fe}_3\text{GeTe}_2$  in-plane magnetocrystalline anisotropy energy is too weak to align the magnetization along its crystalline axes. The softness of the in-plane magnetic anisotropy is further verified by the response of magnetic vortex to an in-plane magnetic field. Because PEEM cannot be operated during application of a magnetic field, we took magnetic images in remanence after applying an in-plane magnetic field pulse. We find that the circulation direction doesn't change until after applying an in-plane magnetic field pulse greater than 120 Oe (Figure 3a). Recalling that vortex circulation can only be changed after the vortex core is pushed out of the circle,<sup>[28]</sup> the result of Figure 3a shows that 120 Oe corresponds roughly the field to saturate the magnetic vortex into a single domain. At 110 K which is below the bulk  $T_C$  of  $\text{Fe}_3\text{GeTe}_2$ , both the Ga implanted and un-implanted area exhibit out-of-plane magnetic stripe domains (Figure 3b) with similar domain width (the greater magnetic contrast in the Ga implanted area is due to the removal of the Pd protection layer by Ga sputtering), proving again our previous assertion that the magnetization in the Ga implanted area is from the majority of Fe rather than from tiny amount of Fe around the implanted Ga atoms. Except the similar out-of-plane magnetic stripe domains, we notice that the Ga implanted circular area still consists of in-plane magnetic component to form a vortex background at zero magnetic field (left in Figure 3b). This result shows that the Ga implantation has already weakened the out-of-plane

magnetic anisotropy at low temperature to tilt the magnetization away from the out-of-plane direction with the out-of-plane component forming the stripe domains and the in-plane component forming a vortex state. Since the formation of a vortex state is due to the magnetic surface charge at the boundary which is proportional to the in-plane magnetization magnitude, the reduced in-plane component at 110 K as compared to that at RT should make the vortex state less favorable. Indeed after applying in-plane magnetic field pulse greater than 60 Oe, the in-plane vortex background has changed to uniform single domain background (Figure 3b) with the out of-plane magnetic stripes unaffected.

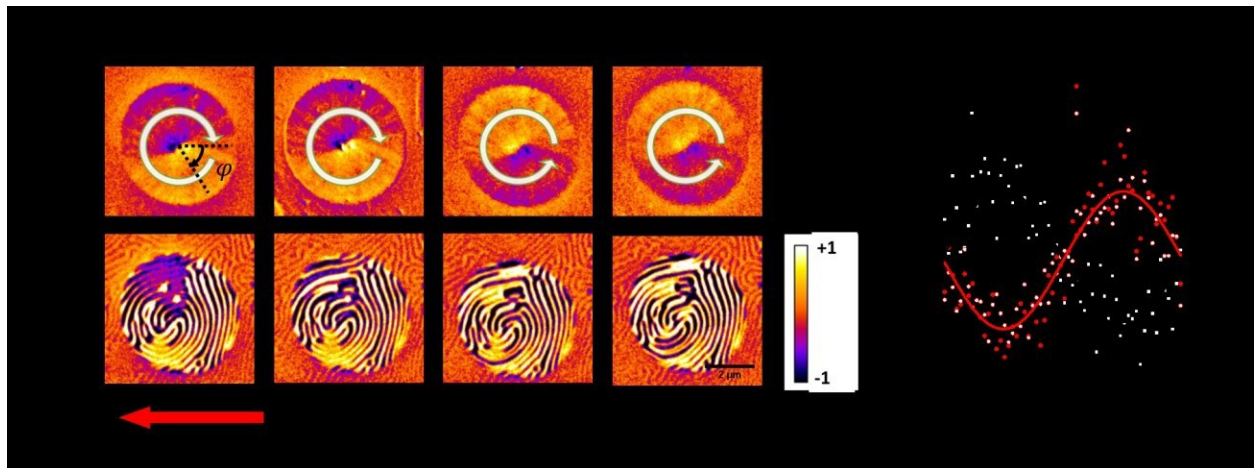


Figure 3. Magnetic domains of a Ga exposed 5- $\mu\text{m}$  diameter circular area after applying magnetic field pulses of 0 Oe, 60 Oe, 120 Oe and 180 Oe at a) RT and b) 110 K. (c) Angular distribution of magnetic contrast from images in a) follows a sinusoidal function, showing the continuous change of magnetization direction within the film plane. Red arrow at the bottom of the figure indicates the incident direction of the circularly polarized x-rays.

In summary, we demonstrate an effective and reliable method to enhance the Curie temperature of  $\text{Fe}_3\text{GeTe}_2$  vdW material by Ga implantation. We show that implanting Ga by the amount of  $10^{-3}\text{Ga } \text{\AA}^{-3}$  and influence of  $\sim 10^{15}$  ions  $\text{cm}^{-2}$  could enhance greatly the

$\text{Fe}_3\text{GeTe}_2$  Curie temperature by  $\sim 100\%$  and far beyond room temperature. In addition, the Ga implantation changes the magnetic anisotropy of  $\text{Fe}_3\text{GeTe}_2$  from out-of-plane at low temperature to in-plane above the bulk Curie temperature. Our result opens up a promising opportunity for tailoring the magnetism of vdW materials above room temperature for future spintronics applications.

## Experimental Section

$\text{Fe}_3\text{GeTe}_2$  is an itinerant vdW ferromagnet with an out-of-plane magnetic anisotropy and a relatively high  $T_C$  ( $\sim 230$  K).<sup>[18,29,30,31,32]</sup> The  $\text{Fe}_3\text{GeTe}_2$  crystal structure is composed of  $\text{Fe}_3\text{Ge}$  layers that are separated by vdW gapped Te double layers (Figure 1a) with the  $\text{Fe}_3\text{Ge}$  containing hexagonal layers of Fe1/Fe1 and Fe2/Ge atoms to form a  $P6_3/mmc$  space group. Because of the weak vdW bonding,  $\text{Fe}_3\text{GeTe}_2$  is easy to be peeled from the bulk crystal using the mechanical exfoliation method.

Thin  $\text{Fe}_3\text{GeTe}_2$  flakes were exfoliated onto a Si(111) substrate from a high-quality bulk  $\text{Fe}_3\text{GeTe}_2$  single crystal which was fabricated by chemical vapor transport method and characterized by superconducting quantum interference device magnetometry.<sup>[14]</sup> To facilitate the  $\text{Fe}_3\text{GeTe}_2$  exfoliation, the sample was heated to  $50^\circ\text{C}$ , exfoliated, and transferred immediately (within 15 minutes) into an ultrahigh vacuum chamber ( $\sim 5 \times 10^{-10}$  Torr). Then a 1.5-nm thick Pd protection layer was grown on top of the sample from a thermal crucible.

Micron sized areas on the  $\text{Fe}_3\text{GeTe}_2$  flake were exposed to the  $\text{Ga}^+$  source (30 kV and 10 pA) of focused ion beam (FIB) instrument (ZEISS CrossBeam 1540 ESB) at the molecular foundry of Lawrence Berkeley National Laboratory. The thicknesses of  $\text{Fe}_3\text{GeTe}_2$  flakes were determined by line scans using atomic force microscopy (AFM). Microscale-resolved mapping of sample strain were acquired by microdiffraction measurements at Beamline 12.3.2 of the Advanced Light Source (ALS), which were performed at  $1\ \mu\text{m}$  per scanning step.<sup>[33]</sup> Magnetic domain images were taken by photoemission electron microscopy

(PEEM) at Beamline 11.0.1 of the ALS using left- and right-circular polarized x-rays at a photon energy of 706.6 eV which corresponds to the energy of maximum x-ray magnetic circular dichroism (XMCD) at Fe  $L_3$  edge. With the incident x-ray at  $60^\circ$  relative to the surface normal direction, our PEEM images are sensitive to both in-plane and out-of-plane magnetizations because the XMCD effect measures the projection of magnetization along the x-ray beam direction.<sup>[34]</sup>

### **Supporting Information**

Supporting Information is available from the Wiley Online Library or from the author.

### **Acknowledgements**

Mengmeng Yang and Qian Li contributed equally to this work. This work is supported by US Department of Energy, Office of Science, Office of Basic Energy Sciences, Materials Sciences and Engineering Division under Contract No. DE-AC02-05CH11231 (van der Waals heterostructures program, KCWF16), National Science Foundation Grant No. DMR-1504568, Future Materials Discovery Program through the National Research Foundation of Korea (No. 2015M3D1A1070467), Science Research Center Program through the National Research Foundation of Korea (No. 2015R1A5A1009962), the KIST Institutional Program, and the National Research Foundation of Korea (No. 2019K1A3A7A09033388). The operations of the Advanced Light Source at Lawrence Berkeley National Laboratory are supported by the Director, Office of Science, Office of Basic Energy Sciences, and U.S. Department of Energy under Contract No. DE-AC02-05CH11231. Work at the Molecular Foundry was supported by the Office of Science, Office of Basic Energy Sciences, of the U.S. Department of Energy under Contract No. DE-AC02-05CH11231.

### **Conflict of interests**

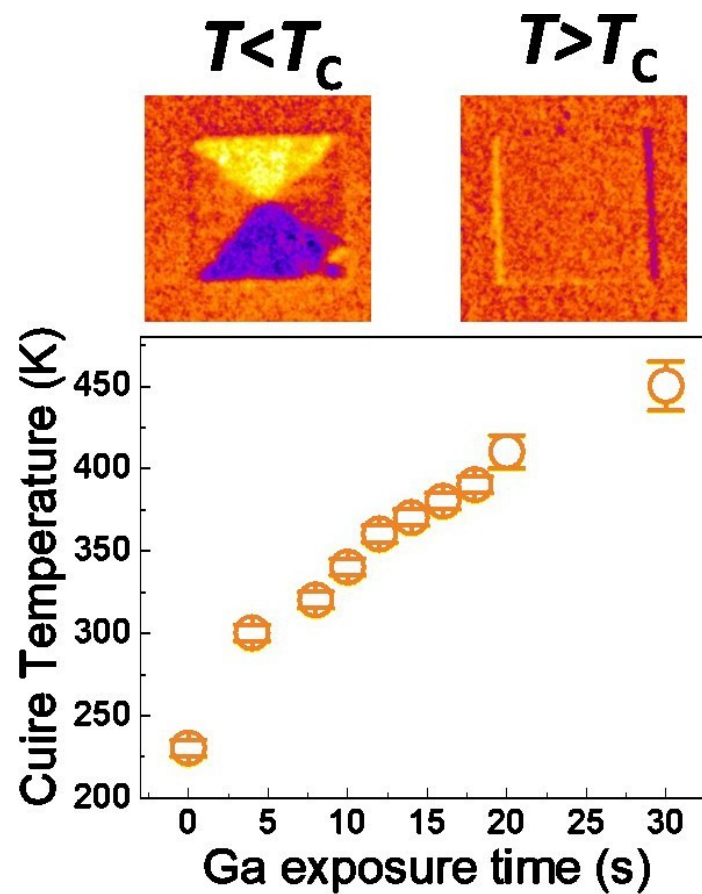
The authors declare no conflict of interest.

### **References**

## Table of Contents

An effective and reliable method of increasing the Curie temperature of ferromagnetic  $\text{Fe}_3\text{GeTe}_2$  van der Waals materials by Ga implantation is reported. Implanting Ga by the amount of  $10^{-3} \text{ Ga } \text{\AA}^{-3}$  could greatly enhance the  $\text{Fe}_3\text{GeTe}_2$  Curie temperature by almost 100%. This result opens a new opportunity for tailoring the magnetic properties of van der Waals materials beyond room temperature.

**Keyword** Curie temperature  
enhancement ToC figure



- 
- [1] C. Gong, L. Li, Z. Li, H. Ji, A. Stern, Y. Xia, T. Cao, W. Bao, C. Wang, Y. Wang, Z. Q. Qiu, R. J. Cava, S. G. Louie, J. Xia, X. Zhang, *Nature* **2017**, 546, 265.
- [2] B. Huang, G. Clark, E. N. Moratalla, D. R. Klein, R. Cheng, K. L. Seyler, D. Zhong, E. Schmidgall, M. A. McGuire, D. H. Cobden, W. Yao, D. Xiao, P. J. Herrero, X. Xu, *Nature* **2017**, 546, 270.
- [3] C. Gong, X. Zhang, *Science* **2019**, 363, eaav4450.
- [4] K. S. Burch, D. Mandrus, J. G. Park, *Nature* **2018**, 563, 47.

- [5] B. Huang, G. Clark, D. R. Klein, D. MacNeill, E. N. Moratalla, K. L. Seyler, N. Wilson, M. A. McGuire, D. H. Cobden, D. Xiao, W. Yao, P. J. Herrero, X. Xu, *Nat. Nanotech.* **2018**, *13*, 544.
- [6] S. Jiang, J. Shan, K. F. Mak, *Nat. Mater.* **2018**, *17*, 406.
- [7] S. Jiang, L. Li, Z. Wang, K. F. Mak, J. Shan, *Nat. Nanotech.* **2018**, *13*, 549.
- [8] Z. Wang, T. Zhang, M. Ding, B. Dong, Y. Li, M. Chen, X. Li, J. Huang, H. Wang, X. Zhao, Y. Li, D. Li, C. Jia, L. Sun, H. Guo, Y. Ye, D. Sun, Y. Chen, T. Yang, J. Zhang, S. Ono, Z. Han, Z. Zhang, *Nat. Nanotech.* **2018**, *13*, 554.
- [9] Y. Sun, R. C. Xiao, G. T. Lin, R. R. Zhang, L. S. Ling, Z. W. Ma, X. Luo, W. J. Lu, Y. P. Sun, Z. G. Sheng, *Appl. Phys. Lett.* **2018**, *112*, 072409.
- [10] Z. Lin, M. Lohmann, Z. A. Ali, C. Tang, J. Li, W. Xing, J. Zhong, S. Jia, W. Han, S. Coh, W. Beyermann, J. Shi, *Phys. Rev. Mater.* **2018**, *2*, 051004(R).
- [11] M. Bonilla, S. Kolekar, Y. Ma, H. C. Diaz, V. Kalappattil, R. Das, T. Eggers, H. R. Gutierrez, M. H. Phan, M. Batzill, *Nat. Nanotech.* **2018**, *13*, 289.
- [12] D. J. O'Hara, T. Zhu, A. H. Trout, A. S. Ahmed, Y. K. Luo, C. H. Lee, M. R. Brenner, S. Rajan, J. A. Gupta, D. W. McComb, R. K. Kawakami, *Nano. Lett.* **2018**, *18*, 3125.
- [13] Y. Deng, Y. Yu, Y. Song, J. Zhang, N. Z. Wang, Z. Sun, Y. Yi, Y. Z. Wu, S. Wu, J. Zhu, J. Wang, X. H. Chen, Y. Zhang, *Nature* **2018**, *563*, 94.
- [14] Q. Li, M. Yang, C. Gong, R. V. Chopdekar, A. T. N'Diaye, J. Turner, G. Chen, A. Scholl, P. Shafer, E. Arenholz, A. K. Schmid, S. Wang, K. Liu, N. Gao, A. S. Admasu, S. W. Cheong, C. Hwang, J. Li, F. Wang, X. Zhang, Z. Q. Qiu, *Nano Lett.* **2018**, *18*, 5974.
- [15] J. Kotakoski, C. Brand, Y. Lilach, O. Cheshnovsky, C. Mangler, M. Arndt, J. C. Meyer, *Nano Lett.* **2015**, *15*, 5944.
- [16] B. S. Archanjo, A. P. M. Barboza, B. R. A. Neves, L. M. Malard, E. H. M. Ferreira, J. C. Brant, E. S. Alves, F. Plentz, V. Carozo, B. Fragneaud, I. O. Maciel, C. M. Almeida, A. Jorio, C. A. Achete, *Nanotechnology* **2012**, *23*, 255305.
- [17] H. Xu, S. Wang, J. Ouyang, X. He, H. Chen, Y. Li, Y. Liu, R. Chen, J. Yang, *Sci. Rep.* **2019**, *9*, 15219.
- [18] H.-J. Deiseroth, K. Aleksandrov, C. Reiner, L. Kienle, R. K. Kremer, *Eur. J. Inorg. Chem.* **2006**, *2006*, 1561.
- [19] Y. Huh, Ki Jung Hong, and Kwang Soo Shin, *Microsc. Microanal.* **2013**, *19*, 33–37.

- [20] W. Scholz, K. Yu Guslienko, V. Novosad, D. Suess, T. Schrefl, R. W. Chantrell, and J. Fidler, *J. Magn. Magn. Mater.* **2003**, *266*, 155.
- [21] H. L. Zhuang, P. R. C. Kent, and R. G. Hennig, *Phys. Rev. B* **2016**, *93*, 134407.
- [22] S. Gautam, S. N. Kane, B.-G. Park, J.-Y. Kim, L. K. Varga, J.-H. Song, K. H. Chae, *J. Non-Cryst. Solids*, **2011**, *357*, 2228.
- [23] D. H. Kim, H. J. Lee, G. Kim, Y. S. Koo, J. H. Jung, H. J. Shin, J.-Y. Kim, J.-S. Kang, *Phys. Rev. B* **2009**, *79*, 033402.
- [24] Cheng Tang, Ling Zhong, Bingsen Zhang, Hao-Fan, Wang, Qiang Zhang, *Adv. Mater.* **2018**, *30*, 1705110.
- [25] Daniel Rhodes, Sang Hoon Chae, Rebeca Ribeiro-Palau, and James Hone, *Nat. Mat.* **2019**, *18*, 541.
- [26] Q. Wang, Q. Zhang, X. Zhao, X. Luo, C. P. Y. Wong, J. Wang, D. Wan, T. Venkatesan, S. J. Pennycook, K. P. Loh, G. Eda, and A. T. S. Wee, *Nano Lett.* **2018**, *18*, 6898.
- [27] H. Ohldag, A. Scholl, F. Nolting, E. Arenholz, S. Maat, A. T. Young, M. Carey, and J. Stöhr, *Phys. Rev. Lett.* **2003**, *91*, 017203.
- [28] M. Urbánek, V. Uhlíř, C.-H. Lambert, J. J. Kan, N. Eibagi, M. Vaňatka, L. Flajšman, R. Kalousek, M.-Y. Im, P. Fischer, T. Šikola, E. E. Fullerton, *Phys. Rev. B* **2015**, *91*,
- [29] B. Chen, J. Yang, H. Wang, M. Imai, H. Ohta, C. Michioka, K. Yoshimura, M. Fang, *J. Phys. Soc. Jpn.* **2013**, *82*, 124711.
- [30] A. F. May, S. Calder, C. Cantoni, H. Cao, M. A. McGuire, *Phys. Rev. B* **2016**, *93*, 014411.
- [31] S. Liu, X. Yuan, Y. Zou, Y. Sheng, C. Huang, E. Zhang, J. Ling, Y. Liu, W. Wang, C. Zhang, J. Zou, K. Wang, F. Xiu, *2D Mater. Appl.* **2017**, *1*, 30.
- [32] Z. Fei, B. Huang, P. Malinowski, W. Wang, T. Song, J. Sanchez, W. Yao, D. Xiao, X. Zhu, A. F. May, W. Wu, D. H. Cobden, J.-H. Chu, X. Xu, *Nat. Mater.* **2018**, *17*,
- [33] M. Kunz, N. Tamura, K. Chen, A. A. MacDowell, R. S. Celestre, M. M. Church, S. Fakra, E. E. Domning, J. M. Glossinger, J. L. Kirschman, G. Y. Morrison, D. W. Plate, B. V. Smith, T. Warwick, V. V. Yashchuk, H. A. Padmore, E. Ustundag, *Rev. Sci. Instrum.* **2009**, *80*, 035108.



---

[34] J. Stöhr, H. C. Siegmann, *Magnetism: From Fundamentals to Nanoscale Dynamics*, Springer, Berlin, Germany **2006**.